A quantitative study of the effect of proton beam intensity on helium, nitrogen and krypton gas target systems

H. Hassani Bidaroni[1], D. Sardari[2] , M. Mirzaee[3], F. Moattar[4]

[1]Department of Energy and Environment, Science and Research Branch, Islamic Azad University,Tehran, 14778, Iran, Email: homayun_hb67@yahoo.co.in
[2]Department of Nuclear Engineering, Science and Research Branch, Islamic Azad University,Tehran, 14515-775, Iran, Email: dariush.sardari@gmail.com
[3]Nuclear Medicine Research Group, Agricultural - Medical and Industrial Research School (AMIRS), Karaj, Iran Email: mohammad.mirzaii.nm@gmail.com
[4]Department of Energy and Environment, Science and Research Branch, Islamic Azad University,Tehran, 14778, Iran, Email: f.moattar@gmail.com

Abstract: We have studied the effect of beam intensity on physical properties of gas target. The high-energy proton beam (12 µA) which was produced in cyclotron of nuclear medicine research group at the Agricultural, Medical and Industrial Research School (AMIRS) entered a conical stainless steel target chamber through a titanium double window. CFD has been used for numerical study of thermal field inside the gas target for three different cases of helium, nitrogen and krypton. The results of both numerical and experimental investigations reveal that target pressure and temperature increase with increasing the beam intensity. Target pressure increasing rate, raises with increasing of gas molecular weight (Kr>N_2>He).
[H. Hassani Bidaroni, D. Sardari, M. Mirzaee, F. Moattar. **A quantitative study of the effect of proton beam intensity on helium, nitrogen and krypton gas target systems.** *Life Sci J* 2012;9(4):4981-4985] (ISSN:1097-8135). http://www.lifesciencesite.com. 746

Keywords: Gambit code; Radioisotope production; gas expansion; proton beam

1. Introduction

Radionuclides are used in nuclear medicine therapy (Chatal and Cornelis, 1999). The principal applications of radionuclides are positron emission tomography (PET), single photon emission computed tomography (SPECT) imaging, radiotherapy and tracing. A summary of typical radionuclides used for internal radiotherapy and their applications are illustrated in Table 1(IAEA Tech. report No. 465).

Table 1. Radionuclides and their applications in internal radiotherapy

Radionuclide	Type of emitter	Half life	Application
^{11}C	Positron emitter	20.3 min	PET imaging
^{13}N	Positron emitter	10 min	PET imaging, Cardiac blood flow agent
^{123}I	159-KeV gamma emitter	13.1 h	SPECT imaging
^{186}Rh	1-MeV beta emitter and 140-KeV gamma emitter	90 h	Radiotoxic therapy

In the 1930's, Lawrence et al., constructed the first cyclotron for examining nuclear reactions and production of radionuclides. Modern radionuclide production apparatus consists of a cyclotron in the energy range 10–30 MeV and a current of up to 350 µA (Bechtold, 1992). The high-energy beam produced in the cyclotron enters the target chamber filled with target gas. The most important experimental investigations on the cyclotron production of radionuclides are summarised in Table 2.

The physical properties (temperature and pressure) and geometrical configuration of the target are important parameters that influence the properties and quantity of the produced radionuclides (Vandecaasteele et al., 1981; Acerbi et al., 1981; Gindler et al., 1976; Helus et al., 1980 and Wojciechowski et al., 1988).

A few numerical studies have investigated the physical properties of target gas properties. For example, Lenz et al., (2011) used computational fluid dynamics (CFD) modelling for simulation of a 200kPa nitrogen target gas. For a better understanding of hydrodynamic motion and physical structure of argon and xenon gases in a GSI_RFQ beam target system, Schneider and Maruhn (1989) performed a numerical simulation of hydrodynamic flow in a cylindrical target gas.

The aim of this study is to evaluate the influence of irradiation intensity on gaseous target pressure and temperature in order to determine the operating constraints for beam intensity and target gas pressure required to prevent the destruction of titanium double windows. CFD modelling was used for numerical modelling of the target gas pressure for a stationary target system.

Table2. Cyclotron produced radionuclides

Authors	Radionuclide	Beam energy
T. J. Ruth et al., 1985	$^{11}CO_2$ and ^{18}F	500 MeV
V. Tolmachev et al., 2000	^{114m}In	12.6 MeV
C. Manuel et al., 1982	^{128}Cs	67 MeV
J. Zweit et al., 1987.	^{66}Ga	31 MeV
E. Joachim et al., 2000	^{124}I	14 MeV
Yevgeny A. et al., 1997	^{153}Gd, ^{188}W, ^{63}Ni, ^{51}Cr and ^{89}Sr	14 MeV
Khandaker M. U. et al., 2010	$^{100g+m,101m,105g+m}Rh$	40 MeV
H. Thisgaard and M. Jensen, 2009	^{119}Sb	low energy

Experimental

The experimental apparatus used in this study is shown in Figures 1 and 2. A stainless steel target chamber with a conical shape (length: 251 mm, front diameter: 17 mm and rear diameter: 38 mm) was designed for the production of radionuclides from helium, nitrogen and krypton gases. A high-energy proton beam (12 μA) produced in the cyclotron at Agricultural, Medical and Industrial Research School (AMIRS) entered the target chamber through double titanium windows of thickness 20 μm. The gap between the titanium windows was cooled using an air stream. After the completion of energy transfer to the gas molecules, the high-energy protons came to a stop at the end of the target chamber. During the irradiation process, the external body of the target was cooled using circulating water at 295 K. The irradiation process was performed in the AMIRS 30-MeV cyclotron using a focused 26.5-MeV proton beam. An ammeter was used to monitor the beam current.

The experimental investigation was performed as follows:

1. A vacuum (10^{-5} mbar) was created inside the chamber.
2. The chamber was filled with the target gas up to an adjusted initial pressure.
3. The target chamber was cooled using circulating water.
4. The target gas was irradiated with a proton beam for 1–2 h.
5. After completion of the irradiation process, the target gas was recovered via a cryogenic vessel.
6. The target pressure and temperature were recorded.
7. The target wall was steam washed.
8. The condensed water contains radionuclides was collected and transferred to a receiving vessel in a hot cell.
9. As described above, three different target gases (helium, nitrogen and krypton) were used for the production of radionuclides. Therefore, in each step of the experiment, the target chamber was filled with one of these gases. A PT barometric pressure indicator was installed at the centre of the target. Two thermometers were installed at the ends of target and the temperature was reported as the average reading of two thermometers. The uncertainties in temperature and pressure measurements were 0.05 °C and 100 kPa, respectively.

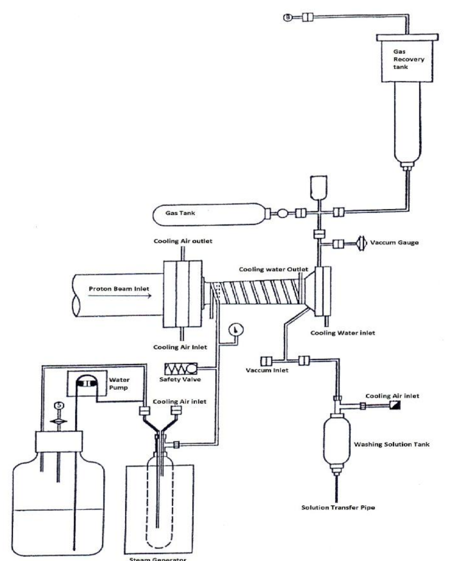

Fig 1. Experimental system

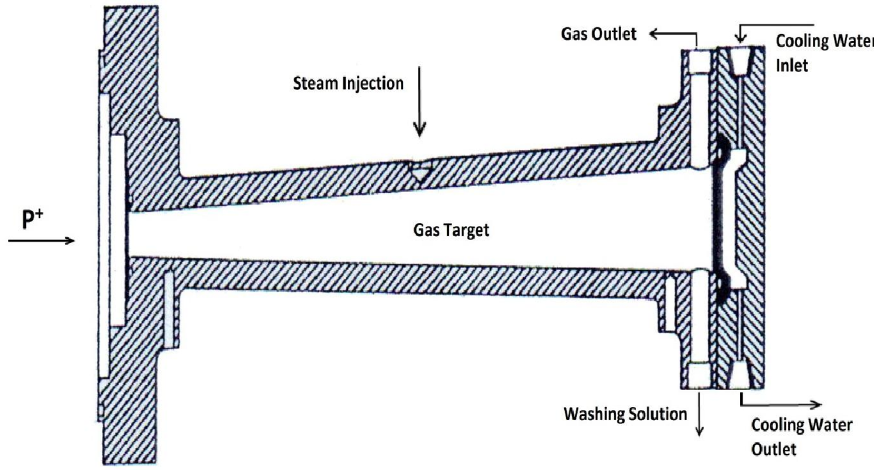

Fig 2. Schematic design of the target gas

CFD modelling

The CFD approach uses a numerical technique for solving the governing equations for a given geometrical and boundary conditions. In this study, the temperature distribution and flow pattern of the target gas inside the target chamber have been simulated using a commercial fluent code version 6.3.

The thermal field of the target gas can be determined by solving the volume-averaged fluid equations for the target gas and cooling fluid sides. The governing equations for the gas and coolant sides include the continuity equation, momentum equation and energy equation as shown below:

1. Continuity equations:

$$coolant\ side;\ \frac{\partial}{\partial x_i}(\rho_w u_i) = 0 \quad (1)$$

$$gas\ side;\ \frac{\partial}{\partial x_i}(\rho_g u_i) = 0 \quad (2)$$

2. Momentum equations:

$$coolant\ side;\ \frac{D}{Dt}(\rho_w u_i) = \frac{-\partial P}{\partial x_i} + \frac{\partial}{\partial x_i}\left(\mu_w \frac{\partial u_i}{\partial x_j}\right) \quad (3)$$

$$gas\ side;\ \frac{D}{Dt}(\rho_g u_i) = \frac{-\partial P}{\partial x_i} + \frac{\partial}{\partial x_i}\left(\mu_g \frac{\partial u_i}{\partial x_j}\right) \quad (4)$$

3. Energy equations:

$$coolant\ side;\ \frac{D}{Dt}(\rho_w Cp_w T) = \frac{\partial}{\partial x_j}\left(k_w \frac{\partial T}{\partial x_j}\right) \quad (5)$$

$$gas\ side;\ \frac{D}{Dt}(\rho_g Cp_g T) = \frac{\partial}{\partial x_j}\left(k_g \frac{\partial T}{\partial x_j}\right) + Q'' \quad (6)$$

Where u_i is the fluid velocity (i = 1, 2 and 3), ρ is the density, P is the pressure, T is the temperature, k is the thermal conductivity, Cp is the heat capacity and Q" is the heat flow. The subscripts g and w refer to gas and cooling fluid (water), respectively.

Q" is estimated as follows:

$$Q'' = \frac{Q'}{V_{Frustum}} \quad (7)$$

$$V_{Frustum} = \frac{1}{12}\pi[D_2^2(x+1) - D_1^2(x)] \quad (8)$$

$$x = \frac{LD_2}{D_2 - D_1} \quad (9)$$

Where $V_{Frustum}$ is the volume of the target chamber; D_1, D_2 and L are the front diameter, back diameter and length of cone, respectively. In this equation, Q' is the energy transferred to the target. The coolant is assumed to be an incompressible fluid. The properties of the gas target are estimated using three different correlations as follows:

1. The ideal gas equation of state:

$$PV = nRT \quad (10)$$

2. The van der Waals equation of state:

$$P = \frac{RT}{V-b} - \frac{a}{V^2} \quad (11)$$

$$a = \frac{27}{64}\frac{R^2 T_{critical}^2}{P_{critical}},\ b = \frac{RT_{critical}}{8P_{critical}} \quad (12)$$

3. The Redlickh-Kwong equation of state:

$$P = \frac{RT}{V-b} - \frac{a}{V(V+b)\sqrt{T}} \quad (13)$$

$$a = 0.4278\frac{R^2 T_{critical}^2\sqrt{T_{critical}}}{P_{critical}},\ b = 0.08664\frac{RT_{critical}}{P_{critical}}$$

Where P is the pressure in atm, V is the volume in m^3, T is the temperature in ºK, R is the universal gas constant (J/mol. K), n is the number of gas moles, b is a constant for correcting volume, a is a constant for correcting the attractive potential of molecules and $T_{critical}$ and $P_{critical}$ are the critical pressure and temperature, respectively.

Geometry and boundary conditions

The geometrical configuration of the problem under consideration for CFD simulation is shown in Figure 3. Commercial Gambit version 2.3.16 was used for preparing the mesh of the target geometry. Several non-uniform grid sizes were used to solve the governing equations for examining grid independence and unstructured grid elements relevant to Figure 4, were found to be suitable for the numerical simulation of the problem.

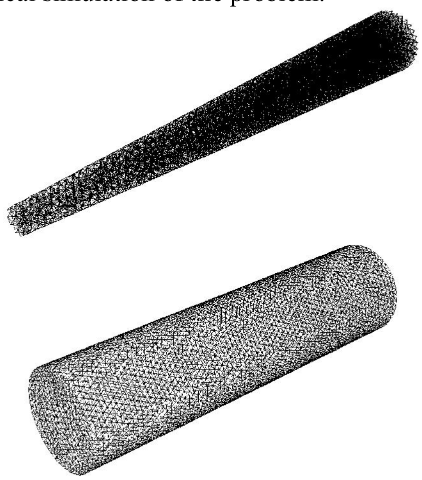

Fig 3. Geometrical configuration of the target gas

A velocity inlet boundary condition (constant velocity and temperature) was used at the target inlet, whereas an outlet flow boundary condition (fully developed flow field) was assumed at the target outlet. No slip conditions or coupled thermal boundary conditions were used at the frustum wall.

The governing equations have been solved iteratively using semi-implicit method (SIMPLE method).

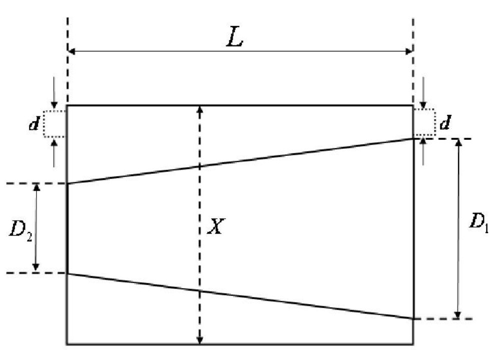

Fig 4. Number of nods in each direction

Results and discussion

Figures 5–9 show the influence of proton beam intensity on the target pressure and temperature of helium, nitrogen and krypton gases. As can be observed, the target pressure increases with increasing beam intensity. There is good agreement between the experimental and CFD results. After beam degradation inside the target and energy transfer to the gas molecules, the target gas temperature increases. Increasing beam intensity causes an increase in beam energy and a resulting increase in target gas temperature and pressure.

The rate of increasing target temperature increases with increasing molecular weight of the target gas (krypton = 83.8, nitrogen = 28 and helium = 4. the maximum increase in the pressure of the krypton target gas is approximately 27% at a beam intensity of 12 µA.

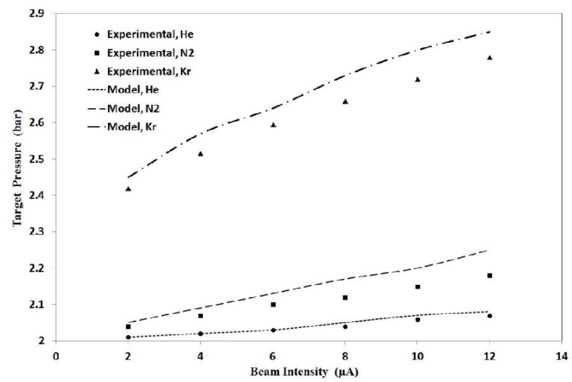

Fig 5. The effect of beam intensity on target gas pressure at P_0=2 bar

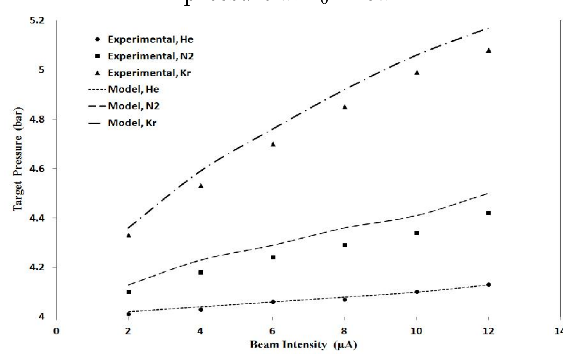

Fig 6. The effect of beam intensity on target gas pressure at P_0=4 bar

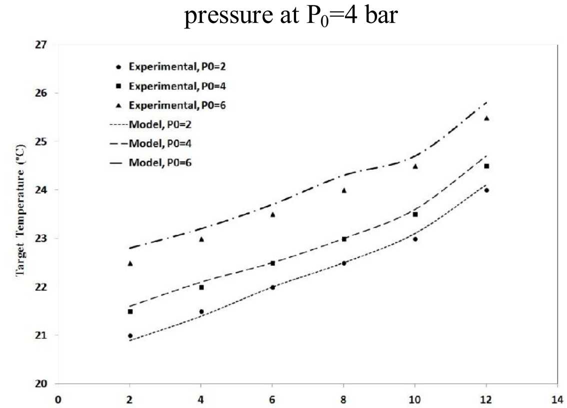

Fig 7. the effect of beam intensity on the helium target gas temperature

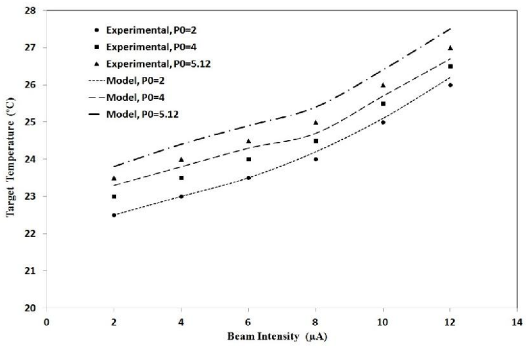

Fig 8. the effect of beam intensity on the nitrogen target gas temperature

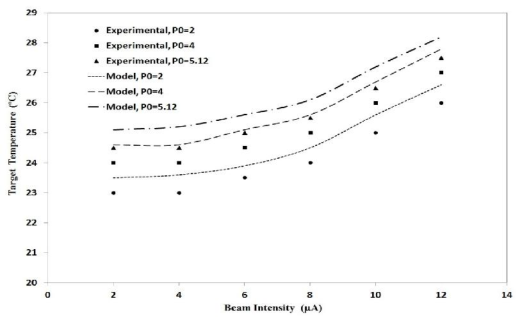

Fig 9. the effect of beam intensity on the krypton target gas temperature

Conclusions:

We study the effect of irradiation intensity on target pressure and temperature. As mentioned above the target pressure increases with the increase in proton beam intensity up to 27% for krypton gas. Titanium double window is affected strongly by the pressure of target gas. Thus operating conditions of target gas should be controlled to prevent physical damages to the titanium windows.

References

1. Chatal, J. F., Hoefnagel, C. A, Radionuclide therapy , The Lancet, Volume 354: 9182, pp. 931-935, 1999.
2. IAEA technical report No. 465, cyclotron produced radionuclides: principles and practices, 2008.
3. V. Bechtold, preceding of the 13th Int. Conf. on cyclotrons and their applications, Vancouver, July 6-10, pp.110, 1992.
4. Lawrence, E.O., Edlefsen, N.E., On the production of high speed protons, Science 72, pp.376–377, 1930.
5. T. J. Ruth, M. J. Adam, J. J. Burgerjon, J. Lenz, B. D. Pate, A gas target for radionuclide production with 500 MeV protons, The International Journal of Applied Radiation and Isotopes, Volume 36:12, pp. 931-933, 1985.
6. Vladimir Tolmachev, Peter Bernhardt, Eva Forssell-Aronsson, Hans Lundqvist, ^{114m}In, a candidate for radionuclide therapy: low-energy cyclotron production and labeling of DTPA-D-Phe-octreotide Nuclear Medicine and Biology, Volume 27: 2, pp.183-188, 2000.
7. Manuel C. Lagunas-Solar, Frank E. Little, Herbert A. Moore Jr., Cyclotron production of ^{128}Cs (3.62 min). A new positron-emitting radionuclide for medical applications, The International Journal of Applied Radiation and Isotopes, Volume 33: 8, pp: 619-628, 1982.
8. J. Zweit, H. Sharma, S. Downey, Production of gallium-66, a short-lived, positron emitting radionuclide, International Journal of Radiation Applications and Instrumentation. Part A. Applied Radiation and Isotopes, Volume 38:7, pp. 499-501, 1987.
9. E. Joachim Knust, Klaus Dutschka, Regin Weinreich, Preparation of 124I solutions after thermodistillation of irradiated 124TeO2 targets, Applied Radiation and Isotopes, Volume 52: 2, pp.181-184, 2000.
10. Yevgeny A. Karelin, Yan N. Gordeev, Vyacheslav T. Filimonov, Yuri G. Toporov, Albert A. Yadovin, Valentin I. Karasev, Vladimir M. Lebedev, Vyacheslav M. Radchenko, Rostislav A. Kuznetsov, Radionuclide production at the Russia State scientific center, RIAR, Applied Radiation and Isotopes, Volume 48: 10-12, pp.1585-1589, 1997.
11. Mayeen Uddin Khandaker, Kwangsoo Kim, Guinyun Kim, Naohiko Otuka, Cyclotron production of the ^{105,106m}Ag, ^{100,101}Pd, ^{100,101m,105}Rh radionuclides by ^{nat}Pd(p,x) nuclear processes, Nuclear Instruments and Methods in Physics Research Section B: Beam Interactions with Materials and Atoms, Volume 268: 14, 15, pp.2303-2311, 2010.
12. H. Thisgaard and M. Jensen, Production of the Auger emitter 119Sb for targeted radionuclide therapy using a small PET-cyclotron, Applied Radiation and Isotopes, Volume 67:1, pp.34-38, 2009.
13. Vandecasteele C. P., Geothals J. S. and Slegers G., Routine production of ^{81}Rb_^{81m}Kr generators using the ^{82}Kr (p, 2n) _^{81}Rb reaction, Radiochem. Radioanal.lett, Vol.46: 285, 1981.
14. Acerbi E., Birattari C., Bonardi M., De martinis C. and Salomone A., Kr (p,x^{n}) excitation functions and ^{81}Rb-^{81m}Kr generator studies, Int.J. Appl. Radio. Isot, Vol32, pp.465-467, 1981.
15. Grindler J. E., Oselka M. C. and friedman A. M., a gas target assembly for the production of high purity, high specific activity ^{81}Rb, Int.J.Appl.Radiat.Isot, Vol 27, 330, 1976.
16. Helus F., Gaspar H. and Sahm U., target system for the routine production of rubidium.81, Radiochem. Radioanal. lett, Vol44, 187, 1980.
17. Wojciechowski P. W., Sajjad M. and Lambrecht R. M., A semi_ quantitative approach to the design, analysis and operation of a gas target system, Appl. Radiat. Isot, Vol39, pp.429-431, 1988.
18. John Lenz and Associates, Gas target coupled density/proton heat load iterative CFD analysis for a ^{124}Xe production target, Nuclear Instruments and Methods in Physics Research Section A: Accelerators, Spectrometers, Detectors and Associated Equipment, In Press, 2011.
19. V. Schneider and J. Maruhn, Simulations of hydrodynamic flow in gas targets irradiated by intense ion beams, Laser and Particle Beams, Vol7, pp.807-828, 1989.

11/4/2012